PNAS RESEARCH ARTICLE | MICROBIOLOGY

Metabolism of host lysophosphatidylcholine in *Plasmodium falciparum*–infected erythrocytes

Jiapeng Liu[a], Katherine R. Fike[a], Christie Dapper[a], and Michael Klemba[a,1]

Edited by L. Sibley, Washington University in St Louis, St. Louis, MO; received November 28, 2023; accepted January 9, 2024

The human malaria parasite *Plasmodium falciparum* requires exogenous fatty acids to support its growth during the pathogenic, asexual erythrocytic stage. Host serum lysophosphatidylcholine (LPC) is a significant fatty acid source, yet the metabolic processes responsible for the liberation of free fatty acids from exogenous LPC are unknown. Using an assay for LPC hydrolysis in *P. falciparum*–infected erythrocytes, we have identified small-molecule inhibitors of key in situ lysophospholipase activities. Competitive activity-based profiling and generation of a panel of single-to-quadruple knockout parasite lines revealed that two enzymes of the serine hydrolase superfamily, termed exported lipase (XL) 2 and exported lipase homolog (XLH) 4, constitute the dominant lysophospholipase activities in parasite-infected erythrocytes. The parasite ensures efficient exogenous LPC hydrolysis by directing these two enzymes to distinct locations: XL2 is exported to the erythrocyte, while XLH4 is retained within the parasite. While XL2 and XLH4 were individually dispensable with little effect on LPC hydrolysis in situ, loss of both enzymes resulted in a strong reduction in fatty acid scavenging from LPC, hyperproduction of phosphatidylcholine, and an enhanced sensitivity to LPC toxicity. Notably, growth of XL/XLH-deficient parasites was severely impaired when cultured in media containing LPC as the sole exogenous fatty acid source. Furthermore, when XL2 and XLH4 activities were ablated by genetic or pharmacologic means, parasites were unable to proliferate in human serum, a physiologically relevant fatty acid source, revealing the essentiality of LPC hydrolysis in the host environment and its potential as a target for anti-malarial therapy.

malaria | lysophospholipid | lysophospholipase | serine hydrolase | fatty acid

Significance

Plasmodium falciparum causes malaria while replicating in host erythrocytes and relies on scavenging rather than de novo synthesis to satisfy its need for fatty acids. Lysophosphatidylcholine (LPC) is an abundant host serum lipid and provides fatty acids and choline for parasite lipid synthesis. In this study, we identify two enzymes of the serine hydrolase superfamily that together are responsible for the metabolism of exogenous LPC. Their loss substantially diminishes the parasite's ability to scavenge fatty acids from LPC and enhances LPC toxicity. Significantly, parasites deficient in LPC hydrolysis are unable to replicate when cultured with human serum, suggesting that LPC metabolism could be targeted as an anti-malarial strategy.

Malaria counts among the most devastating infectious diseases in the world today. An estimated 247 million cases and 619,000 deaths were attributed to malaria in 2021 (1). Continued development of new anti-malarial strategies will be required to mitigate the effects of eventual drug resistance against current frontline therapies (2).

During the pathogenic, asexual stage of the human malaria parasite *Plasmodium falciparum* within erythrocytes, high rates of phospholipid synthesis are required to support the expansion of parasite membranes (3). Parasites also produce the neutral lipids diacylglycerol (DAG) and triacylglycerol (TAG), which are deposited in lipid droplets and are mobilized late in the replication cycle (4, 5). Although the *P. falciparum* genome encodes enzymes for de novo fatty acid (FA) synthesis, these are dispensable in the asexual stage (6). Thus, the intraerythrocytic parasite is dependent on exogenous sources of fatty acids to support its vigorous anabolic activity. Host serum contains two abundant fatty acid sources: free fatty acids and lysophosphatidylcholines (LPC) (7). LPC consists of a fatty acyl chain (that can vary in length and degree of unsaturation) esterified to glycerophosphocholine and is transported through the circulation as a complex with serum albumin (8). Studies with isotope-labeled LPC have demonstrated that LPC-derived fatty acids are readily incorporated into parasite lipids (9, 10). Furthermore, LPC can support parasite growth as the sole source of exogenous fatty acids (11). LPC catabolism also provides choline (10, 12), an important precursor for phosphatidylcholine (PC) biosynthesis. While the metabolites supplied by LPC catabolism support asexual growth, the depletion of this host lipid plays a regulatory role by enhancing commitment to gametocytogenesis (10).

It has long been evident that asexual *P. falciparum* exhibits high levels of A-type lysophospholipase activity, which generates free fatty acids and glycerophosphocholine from LPC (13). While the identity of the enzyme(s) responsible for this activity is unknown, members of the serine hydrolase superfamily are likely candidates, based on the well-established esterase and thioesterase activities of mammalian lysophospholipases A1 and A2 (14). Deletion of both enzymes in Neuro2A cells resulted in elevated LPC levels, which suggests that their lysophospholipase activities are physiologically relevant (15). Two chemoproteomic studies have identified 29 serine hydrolases that are expressed during

Author affiliations: [a]Department of Biochemistry, Virginia Tech, Blacksburg, VA 24061

Author contributions: J.L. and M.K. designed research; J.L., K.R.F., and C.D. performed research; J.L., K.R.F., C.D., and M.K. analyzed data; and J.L. and M.K. wrote the paper.

The authors declare no competing interest.

This article is a PNAS Direct Submission.

[1]To whom correspondence may be addressed. Email: klemba@vt.edu.

This article contains supporting information online at https://www.pnas.org/lookup/suppl/doi:10.1073/pnas.2320262121/-/DCSupplemental.

Published February 13, 2024.

the asexual development of *P. falciparum* (16, 17). Three of these enzymes, termed PfLPL1, PfLPL3, and PfLPL20, have been shown to have lysophospholipase activity in vitro and PfLPL3 contributed to the hydrolysis of a fluorescent LPC analog in the parasitophorous vacuole (18–20). At this time, the number of lysophospholipases expressed in the asexual parasite, and their relative contributions to exogenous LPC hydrolysis, remain to be clearly defined.

To expedite the discovery of key parasite lysophospholipases, we have pursued complementary chemical biology and genetic approaches. We first developed an assay for in situ LPC hydrolysis that enabled the identification of serine hydrolase inhibitors that block the release of fatty acids from LPC (here, in situ refers to processes in intact, infected erythrocytes in culture). Candidate lysophospholipases were interrogated by activity-based protein profiling, leading to a serine hydrolase subgroup consisting of four paralogs. Single and multigenic knockout parasite lines were generated to characterize their roles individually and in combination. Two of these four enzymes were revealed to be the source of nearly all LPC-hydrolyzing activity in asexually replicating parasites. The consequences of the loss of these activities on the ability of parasites to scavenge fatty acids from LPC and to survive in high-LPC environments were investigated.

Results

Parasite Serine Hydrolases Catalyze LPC Hydrolysis In Situ. To gain insight into key lysophospholipase activities, we sought to identify serine hydrolase-directed, small-molecule inhibitors of LPC hydrolysis in situ. We developed an approach based on a quantitative, intact-cell assay for the incorporation of a fluorescent fatty acid analog, BODIPY™ 500/510 C_4, C_9 (C4,C9-FA), into parasite neutral lipids with BODIPY-TR-ceramide (BTC) serving as an internal standard for normalization (21). We reasoned that unlabeled fatty acids derived from LPC hydrolysis would compete with C4,C9-FA and thereby reduce lipid-associated fluorescence. To test this, C4,C9-FA labeling of the neutral lipids diacylglycerol (DAG) and triacylglycerol (TAG) in cultured parasites was examined in the presence of exogenous LPC 18:1 (Fig. 1*A*). LPC reduced C4,C9-FA incorporation in a concentration-dependent manner, while a non-hydrolysable LPC analog (lyso-platelet activating factor 18:1) was ineffective (Fig. 1*A*). These findings demonstrate that LPC hydrolysis is required for suppression of C4,C9-FA labeling and that LPC/C4,C9-FA mixtures can serve as the basis of an assay for inhibition of in situ lysophospholipase activities.

We next tested a panel of serine hydrolase inhibitors for the ability to block LPC hydrolysis as reflected by a gain in C4,C9-FA labeling of DAG and TAG (Fig. 1 *B* and *C*). These inhibitors included: 1) isopropyldodecyl fluorophosphonate (IDFP), a monoacylglycerol isostere and potent lipase inhibitor (22) that we have previously employed to identify putative *P. falciparum* lipases (17); 2) JW642, a monoacylglycerol lipase inhibitor (23) that inhibits an abundant *P. falciparum* serine hydrolase and putative lipase termed "prodrug activating and resistance esterase" (PfPARE) (17); and 3) a panel of highly potent, structurally diverse, inhibitors of mammalian monoacylglycerol lipase that are based on a piperazine- or piperadine-urea scaffold (24) (see Fig. 1*D* and *SI Appendix*, Fig. S1*A* for compound structures). All inhibitors act through a competitive-covalent mechanism by reacting with the active site serine residue and were assayed at 10 μM concentration. Only two inhibitors, IDFP and AKU-010, elicited a strong recovery of C4,C9-FA lipid labeling (Fig. 1*C*). The AKU-010 analogs AKU-005 and AKU-006 exhibited modest and no inhibition of LPC hydrolysis, respectively, and JW642 did not inhibit LPC hydrolysis. To control for the effects of inhibitors on C4,C9-FA uptake and DAG and TAG labeling per se, the screen was repeated in the absence of LPC (*SI Appendix*, Fig. S1*B*). While some inhibitors caused a modest decrease in label incorporation relative to vehicle control, this effect did not account for the suppression of labeling observed in the presence of LPC and AKU-005, AKU-006, or JW642. A statistical test demonstrated that label incorporation in the presence of AKU-010 was unaffected by LPC, in contrast to the other analogs tested (*SI Appendix*, Fig. S1*B*). We conclude that AKU-010 acts to inhibit LPC hydrolysis in situ. Furthermore, the compounds AKU-010/005/006/JW642 define an inhibition profile for the dominant *P. falciparum* lysophospholipase activities.

To identify candidate lysophospholipases, we profiled the inhibitor sensitivities of parasite and host serine hydrolases using the activity-based probe TAMRA-fluorophosphonate (TAMRA-FP) (25). To ensure that all enzymes within the infected erythrocyte were included in this analysis, parasitized erythrocytes (infected RBC, or iRBC) were highly enriched by "magnetic activated cell sorting," or MACS (26). The strong labeling of host erythrocyte acylpeptide hydrolase (80 kDa) as well as a parasite-internalized form (55 kD) was suppressed using the APEH-selective inhibitor AA74-1 (27). Profiling of iRBC lysate revealed multiple serine hydrolases for which TAMRA-FP labeling was blocked by AKU-010, and several of these exhibited an inhibitor specificity that matched the in situ profile (Fig. 1*E*). Contrasting with this, none of the host erythrocyte serine hydrolases was inhibited by AKU-010 (Fig. 1*F*), indicating that parasite-encoded enzymes are the key catalysts of LPC hydrolysis in infected erythrocytes.

Two Exported Serine Hydrolases Are Targets of AKU-010. To gain insight into the enzyme(s) responsible for LPC hydrolysis, we consulted our previous proteomic analysis of serine hydrolase-family lipases in *P. falciparum* (17). Of the seven putative lipases identified in that study, one stood out as a top candidate: PF3D7_1001600, previously termed "exported lipase 2" (XL2) based on its export to the host erythrocyte cytosol (28). XL2 has a predicted molecular mass (88.6 kDa) that is consistent with that observed for the major activity in the TAMRA-FP analysis (Fig. 1*E*). A paralog of XL2, termed "exported lipase 1" (XL1; PF3D7_1001400), is also exported to the erythrocyte (28). To determine whether XL1 and XL2 correspond to the AKU-010-sensitive activities, we generated single- and double-knockout parasite lines, targeting the entire coding sequences for deletion using a markerless CRISPR-Cas9 strategy (*SI Appendix*, Fig. S2 *A–E*). The ΔXL1 line appeared to have undergone telomere shortening or "healing," a phenomenon that can occur when double-stranded DNA breaks are made in sub-telomeric regions (29), whereas the ΔXL2 single knockout and the ΔXL1/2 double knockout contained the expected gene deletion events. All knockout lines grew normally in media containing the serum replacement Albumax I, indicating that neither XL1 nor 2 is required under these culture conditions.

TAMRA-FP profiling of the knockout lines revealed that XL1 corresponds to the AKU-010-sensitive activity at ~110 kDa (Fig. 2*A*). XL2 is a highly expressed enzyme that corresponds to three of the AKU-010-sensitive species (Fig. 2*B*); the two smaller species are likely generated by limited proteolytic cleavage. Both proteins are absent from the ΔXL1/2 line (*SI Appendix*, Fig. S2*F*). To establish that endogenous XL1 and XL2 are exported to the host erythrocyte, MACS-enriched wild-type parasites were fractionated with saponin into a supernatant fraction that contains soluble erythrocyte proteins and a pellet fraction that contains

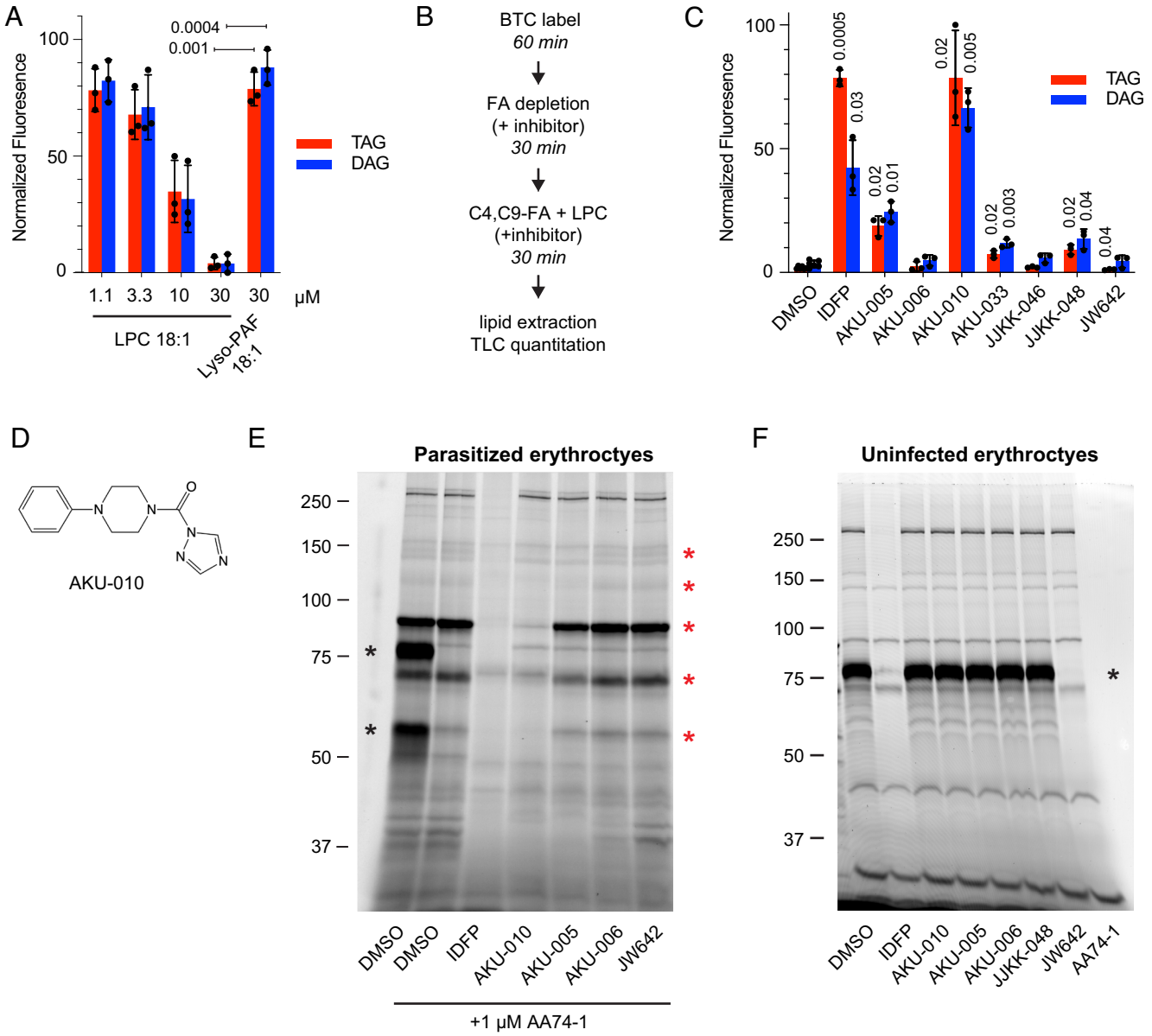

Fig. 1. Serine hydrolase inhibitors block LPC hydrolysis in situ. (*A*) Fatty acids derived from LPC hydrolysis reduce C4,C9-FA incorporation into parasite neutral lipids. LPC or the non-hydrolysable LPC analog lyso-PAF were co-incubated with C4,C9-FA for 30 min and incorporation into DAG and TAG was quantified and normalized to a no-LPC control (set to 100). Means and SD are from three independent experiments. Significance of the differences in the 30 μM LPC and lyso-PAF means was assessed using an unpaired, two-tailed *t*-test with Welch's correction for unequal variance (hereafter referred to as "Welch's *t*-test"); *P*-values for DAG and TAG are indicated. (*B*) C4,C9-FA/LPC competition assay for identifying inhibitors of in situ LPC hydrolysis. BTC, BODIPY-TR-ceramide internal standard; TLC, thin layer chromatography. (*C*) Definition of an inhibition profile for in situ LPC hydrolysis. Inhibitors were evaluated in a C4,C9-FA/LPC competition assay at 10 μM. C4,C9-FA fluorescence intensities were normalized to a no-LPC, no inhibitor control (set to 100). Means and SD are from three independent experiments. Statistical significance (inhibitor vs. DMSO control) was assessed using Welch's *t*-test; *P*-values below 0.05 are displayed above the bars. (*D*) Structure of AKU-010. (*E*) Inhibition of serine hydrolases in lysates of MACS-enriched, *P. falciparum*–infected erythrocytes as assessed by TAMRA-FP profiling. AA74-1 was included to suppress the strong signal from erythrocyte acylpeptide hydrolase (APEH), which was present as 80- and 55-kDa species (far left lane, black asterisks). Red asterisks indicate species with the inhibition profile AKU-010 > AKU-005 >> AKU-006, JW642. (*F*) TAMRA-FP profiling of uninfected erythrocytes. Inhibition of erythrocyte serine hydrolases was only observed with IDFP and AA74-1. Black asterisk, APEH. Sizes of markers are indicated in kDa.

intraparasitic proteins (Fig. 2*C*). Both enzymes were recovered exclusively in the supernatant fraction, confirming efficient export, whereas the intracellular enzyme PfPARE (30) was located in the parasite pellet.

To assess the effects of loss of XL1 and/or 2 on LPC hydrolysis in situ, we modified our fatty acid probe-competition assay by replacing C4,C9-FA with a terminal alkyne analog of oleic acid (oleate alkyne, OA), a probe that more closely resembles the structure of a physiological fatty acid. Parasites were labeled with 30 μM OA with or without 30 μM LPC 18:1 for 40 min. Lipids were extracted from saponin-isolated parasites and alkyne-containing lipids were rendered fluorescent by click addition of 3-azido-7-hydroxycoumarin and resolved by thin-layer chromatography as previously described (31). For the parental 3D7 line, LPC reduced OA labeling to ~30 to 60% of that in its absence (Fig. 2 *D* and *E*). In ΔXL1, ΔXL2, and ΔXL1/2 parasites, no significant changes in OA labeling were observed for PE, DAG, or TAG compared to 3D7 (Fig. 2*E*). In contrast to these lipids, PC labeling was somewhat elevated in ΔXL2 and ΔXL1/2 lines. Overall, these studies revealed that XL1/2-deficient parasites retained the ability to efficiently release fatty acids from LPC.

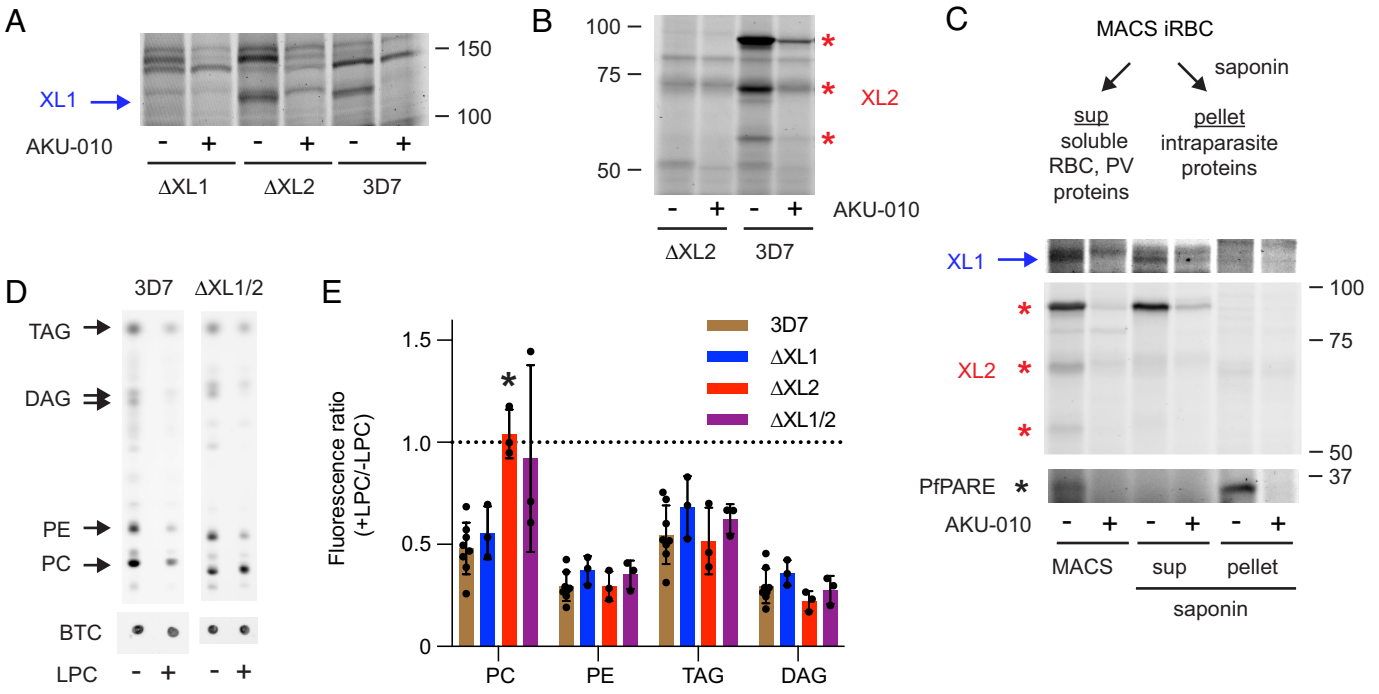

Fig. 2. Two exported serine hydrolases are targets of AKU-010. (*A*) TAMRA-FP profiling of MACS-enriched ΔXL1, ΔXL2, and 3D7 iRBCs. XL1 is indicated with a blue arrow. (*B*) TAMRA-FP profiling of MACS-enriched ΔXL2 and 3D7 iRBCs. Three AKU-010-inhibited species corresponding to XL2 are indicated with red asterisks. (*C*) XL1 and XL2 are exported to the host cell. *Upper*: Schematic for fractionation of MACS-enriched 3D7 parasites into saponin supernatant and pellet fractions. *Lower*: TAMRA-FP labeling reveals that XL1 (blue arrow) and XL2 (red asterisks) appear predominantly in the saponin supernatant containing soluble erythrocyte proteins, whereas the intracellular serine hydrolase PfPARE (black asterisk) appears exclusively in the parasite pellet. In *A*–*C*, sizes of protein standards are given in kDa. In *C*, XL1 migrates between the 100- and 150-kDa markers, similar to *A*. (*D*) Representative thin-layer chromatograms depicting the effects of LPC on incorporation of OA into parasite lipids in 3D7 and ΔXL1/2 parasites. The two DAG species are 1,2- and 1,3-isomers. BTC, BODIPY-TR-ceramide internal standard. Note the differential effect of LPC on OA labeling of PC in the two lines. (*E*) Oleate alkyne/LPC competition profiling of single and double XL1/2 knockout lines. Ratios below 1 (dotted line) indicate suppression of OA incorporation in the presence of LPC. Means and SD are from at least three independent experiments. Significance relative to 3D7 was assessed within lipid groups with Welch's *t*-test. *, $P < 0.05$.

Intracellular and Exported Lysophospholipases Contribute to Efficient LPC Hydrolysis. We reasoned that additional AKU-010-sensitive serine hydrolases were responsible for exogenous LPC hydrolysis in ΔXL1/2 parasites. We focused our attention on two enzymes that have been identified as XL1/2 paralogs in the PlasmoDB database: PF3D7_0731800 and PF3D7_1328500. Neither sequence contains a canonical PEXEL host targeting motif (32) for export to the host erythrocyte (PlasmoDB.org); thus, we refer to these as "exported lipase homolog" (XLH) 3 and 4, respectively.

We first attempted to identify XLH3 in the TAMRA-FP profile of iRBC serine hydrolases by generating a knockout line by marker-free CRISPR/Cas9 deletion (*SI Appendix*, Fig. S3 *A* and *B*). We also generated a yellow fluorescent protein (YFP)-tagged line by single cross-over homologous recombination and selection-linked integration (33) (*SI Appendix*, Fig. S4 *A* and *B*). TAMRA-FP profiling of MACS-enriched iRBCs of the ΔXLH3 and XLH3-YFP parasite lines failed to reveal a labeled species that could be attributed to XLH3. This finding suggests that the protein is not expressed in the asexual stage or is expressed below the detection threshold of our assay, a conclusion that is supported by published transcriptomic and proteomic data indicating low expression in asexual parasites (*SI Appendix*, Table S1). Preliminary OA/LPC competition experiments yielded results essentially identical to those obtained with 3D7; thus, we did not characterize this single-knockout line in detail.

We next generated a parasite line expressing an endogenous XLH4-YFP fusion (*SI Appendix*, Fig. S4*C*). TAMRA-FP profiling revealed a ~30-kDa increase in molecular mass associated with a ~150-kDa serine hydrolase that was partially inhibited by 10 μM AKU-010 in vitro (Fig. 3*A*). Live-cell fluorescence microscopy revealed a diffuse distribution of XLH4-YFP within the parasite (Fig. 3*B*). A similar distribution was observed in aldehyde-fixed parasites expressing XLH4 fused to a triple hemagglutinin (HA) tag (Fig. 3*C*). In both cases, the enzyme was only observed within the confines of the parasitophorous vacuole/plasma membrane in what appears to be a primarily cytosolic distribution. To assess the contribution of XLH4 to LPC hydrolysis, we generated parasite lines in which the XLH4 coding sequence was truncated by homologous recombination to render the enzyme non-functional, yielding single (ΔXLH4), double (ΔXL2/XLH4) and triple (ΔXL1/2/XLH4) knockout lines (*SI Appendix*, Fig. S3 *C*–*E*). Finally, we introduced an XLH3 coding sequence deletion on the ΔXL1/2/XLH4 background to produce a parasite line devoid of all four XL/XLH coding sequences (*SI Appendix*, Fig. S3*F*). The resulting ΔXL1/2/XLH3/4 line is referred to as "quadruple knockout," or QKO. We confirmed the loss of XLH4 in two independently generated lines (ΔXL2/XLH4 and QKO) by TAMRA-FP profiling (Fig. 3*D* and *SI Appendix*, Fig. S3*G*).

OA/LPC competition assays were conducted to determine the contribution of XLH4 to in situ LPC hydrolysis. While loss of XLH4 alone had a minimal effect, deletion of XLH4 on a ΔXL2 background (ΔXL2/XLH4, ΔXL1/2/XLH4, and QKO lines) was associated with a strong reduction of LPC hydrolysis as reflected by increased OA labeling of DAG, TAG and PE (Fig. 3*E*; a +LPC/-LPC ratio of 1 indicates no competition). To our surprise, a ~10-fold increase in the fluorescence ratio for PC was observed with ΔXL1/2/XLH4 and QKO lines over the parental 3D7 line. An increase in PC labeling was also observed with LPC 16:0 but not when LPC was replaced with lysophosphatidylethanolamine, lysophosphatidylserine, or the non-hydrolysable LPC analog

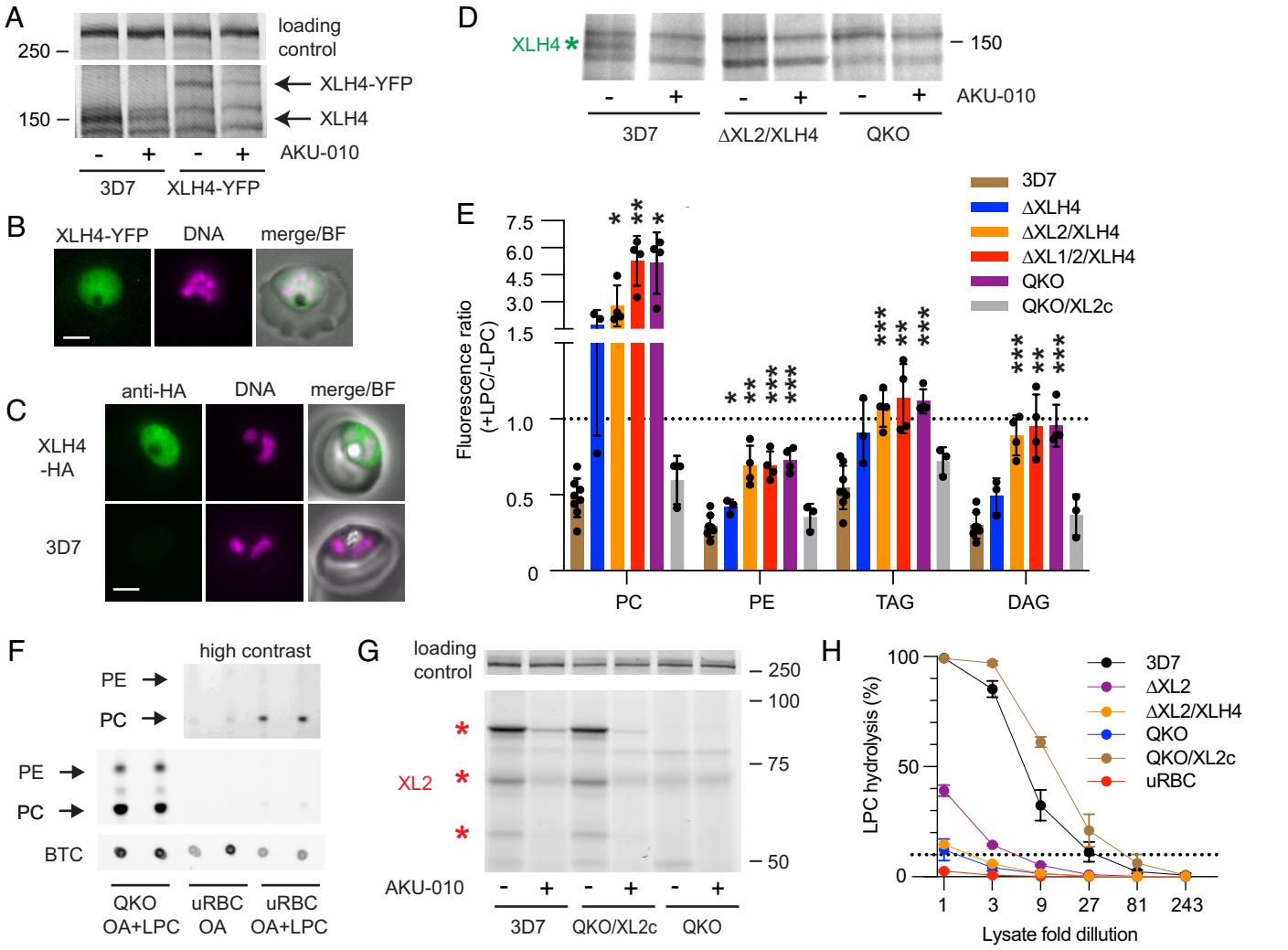

Fig. 3. Exported XL2 and intraparasitic XLH4 govern the metabolism of exogenous LPC in asexual parasites. (*A*) TAMRA-FP profiling of MACS-enriched parental 3D7 and XLH4-YFP-expressing parasites. YFP tagging of XLH4 results in a mass increase of ~30 kDa. A ~270-kDa erythrocyte serine hydrolase, which is not inhibited by AKU-010 (Fig. 1*F*), is shown as a loading control. (*B*) A live parasitized erythrocyte exhibiting intraparasitic XLH4-YFP fluorescence. (*C*) Immunofluorescence localization of XLH4-HA. A 3D7 parasite imaged with identical parameters is shown as a negative control. In *B* and *C*: Hoechst 33342 fluorescence (DNA) is pseudocolored magenta. BF, bright-field. (Scale bar, 3 μm.) (*D*) TAMRA-FP profiling demonstrates the loss of XLH4 (green asterisk) in MACS-enriched double (ΔXL2/XLH4) and quadruple (QKO) knockout lines. Full gel images are shown in *SI Appendix*, Fig. S3*G*. (*E*) Oleate alkyne/LPC competition profiling of XLH4 single and XL/XLH multiple knockout lines. A ratio of 1 (dotted line) indicates no competition from LPC hydrolysis. Means and SD are from at least three independent experiments. Significance relative to 3D7 was assessed within lipid groups with Welch's *t*-test. *, $P < 0.05$; **, $P < 0.01$; ***, $P < 0.001$. (*F*) Enhanced OA labeling of PC in QKO parasites is not due to erythrocyte acyltransferase activity. Equivalent numbers of MACS-enriched QKO iRBC or uninfected erythrocytes (uRBC) were labeled with OA with or without LPC as indicated, in duplicate. Phospholipids were resolved by TLC. (*G*) TAMRA-FP profiling of MACS-enriched parasites reveals comparable XL2 expression in the complemented QKO parasite (QKO/XL2c) and parental 3D7 lines. The loading control is that described in *A*. (*H*) In vitro lysophospholipase activity in lysates of equivalent numbers of MACS-enriched iRBC or uRBC. Percent of TopFluor LPC hydrolysis is shown for serial threefold dilutions of lysates. The dotted line indicates 10% substrate hydrolysis. Means and SD are from three independent experiments.

lyso-PAF (all with 18:1 fatty acyl groups; *SI Appendix*, Fig. S5). The most plausible explanation for this finding is that unhydrolyzed LPC is directly acylated to PC through the activity of an LPC acyltransferase. Because erythrocytes possess LPC acyltransferase activity for the purpose of phospholipid remodeling (i.e., the Lands cycle) (34), we asked whether PC is efficiently formed from OA and LPC in uninfected erythrocytes. While a very small amount of OA-labeled PC was observed, it was insignificant compared to that in QKO parasites (Fig. 3*F*). Thus, the increase in OA label incorporation into PC in XL/XLH-deficient parasites cannot be attributed to a host cell acyl transfer pathway.

Finally, we complemented the QKO line with an XL2 expression cassette delivered on a *piggybac* transposon (*SI Appendix*, Fig. S6). TAMRA-FP profiling indicated that the complemented parasite line, termed QKO/XL2c, expressed XL2 at a comparable level to that of parental 3D7 parasites (Fig. 3*G*). XL2 complementation fully restored the capacity of parasites to efficiently hydrolyze LPC in situ (Fig. 3*E*).

XL2 and XLH4 Catalyze LPC Hydrolysis. To determine whether XL/XLH enzymes directly contribute to LPC metabolism through hydrolysis of the fatty acyl ester via A1-type lipase activity, we developed an in vitro lysophospholipase assay that employs a fluorescent LPC analog, TopFluor-LPC. Lysates of MACS-enriched 3D7, ΔXL2, ΔXL2/XLH4, QKO, and QKO/XL2c parasites, as well as uninfected RBC (uRBC), were generated at equivalent cell densities. Serial threefold dilutions were then assayed for hydrolysis of TopFluor-LPC, with substrate and product (TopFluor-FA) resolved by TLC and quantified by fluorescence scanning (*SI Appendix*, Fig. S7).

Consistent with a previous report (13), lysophospholipase (LPL) activity was greatly elevated in 3D7-infected cells over that

in uRBC (Fig. 3*H*). A substantial drop in LPL activity in the ΔXL2 lysate indicates that much of that activity can be attributed to XL2. Interpolating the dilutions required for 10% substrate hydrolysis, we estimate that loss of XL2 resulted in a ~6-fold reduction in LPL activity. Comparison of ΔXL2 and ΔXL2/XLH4 lysates revealed an additional ~3-fold drop in LPL activity upon loss of XLH4. No further reduction of LPL activity was observed in QKO parasites, indicating that neither XL1 nor XLH3 contributed appreciably to hydrolysis of the TopFluor-LPC substrate. The level of LPL activity was slightly above that of uRBC, which suggests that a small amount of residual activity remains in QKO parasites. XL2 complementation of QKO restored LPL activity to wild-type levels. We conclude that XL2 and XL4 are authentic lysophospholipases and that they constitute the bulk of LPC-hydrolyzing activity in infected erythrocytes.

XL/XLH-Deficient Parasites Cannot Efficiently Use Exogenous LPC as a Source of Fatty Acids and Are Hypersensitive to LPC Toxicity. We expected that the depletion of LPL activities in QKO parasites would impact their ability to scavenge fatty acids from exogenous LPC. To test this, we washed synchronized ring-stage parasites into media containing two LPC species, 16:0 and 18:1, as sole sources of fatty acids ("2LPC medium") at concentrations from 5 to 50 μM each. For normalization, parasites were also cultured with 0.5% Albumax I. Prior studies have reported that palmitic and oleic acids are sufficient to support parasite growth over multiple generations (35, 36); however, we found that only one complete cycle could be sustained in 2LPC medium. Thus, we evaluated parasite proliferation by comparing second-cycle parasitemias, normalizing 2LPC values to those in 0.5% Albumax-containing media.

Second-cycle parasitemias of wild-type 3D7 parasites were optimal at LPC concentrations between 15 and 25 μM each (Fig. 4*A*) and declined at higher concentrations. While elevated LPC concentrations have been reported to perturb erythrocyte membranes (37, 38), we did not observe hemolysis under these conditions. As expected, the second-cycle parasitemias of QKO parasites in 2LPC medium were significantly diminished at all LPC concentrations (Fig. 4*A*); however, some parasite development remained at 15 to 25 μM concentrations. Notably, XL2 complementation of the QKO line restored robust growth in 2LPC media (Fig. 4*A*).

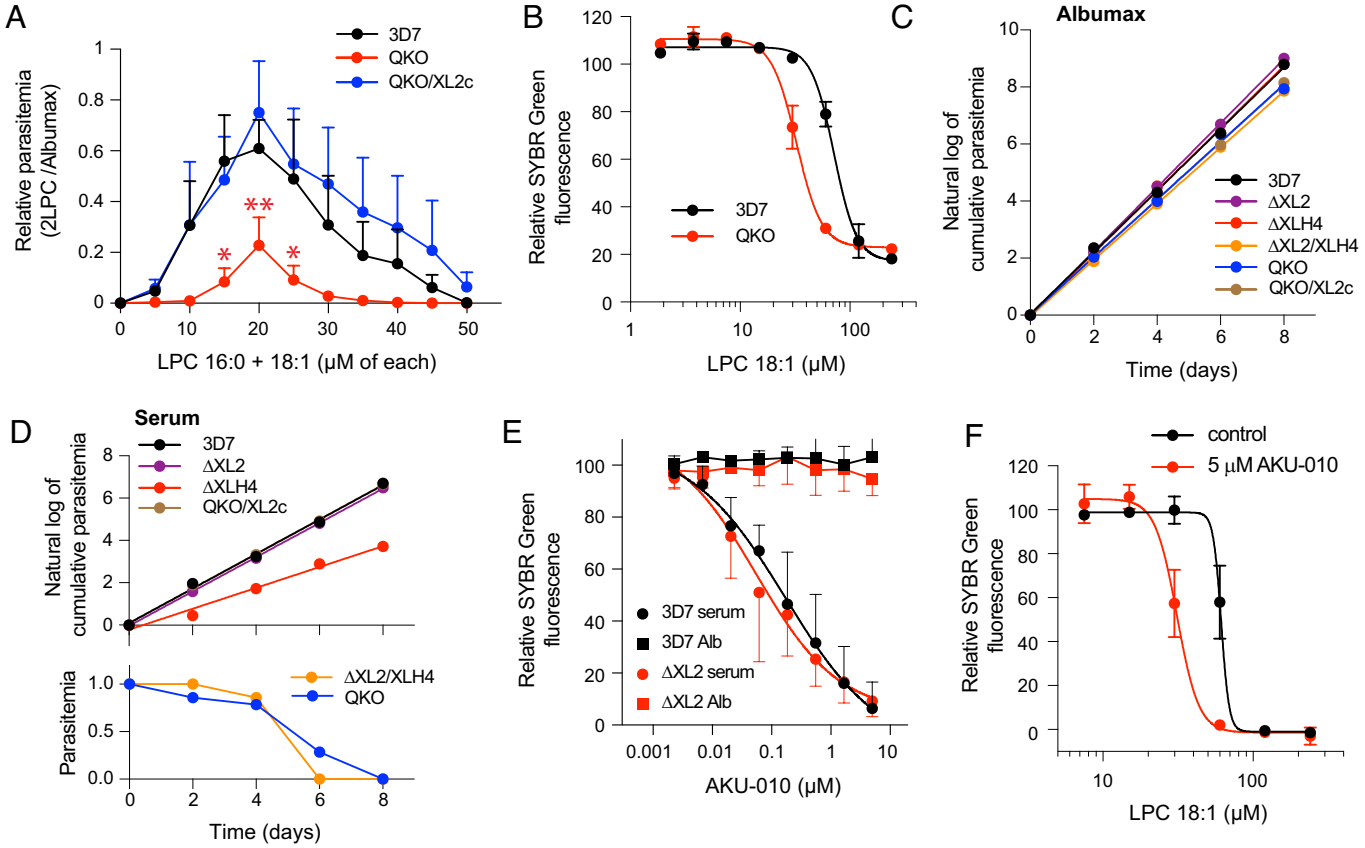

Fig. 4. Loss of XL2 and XLH4 activities impairs fatty acid scavenging from LPC, exacerbates LPC toxicity, and abrogates growth in serum. (*A*) QKO parasites have diminished ability to use LPC as a sole source of fatty acids. Ring-stage parasites were cultured for one generation in a minimal-lipid medium containing the indicated range of concentrations of each of LPC 16:0 and 18:1 ("2LPC") or in standard culture medium containing 0.5% Albumax. Relative parasitemias were calculated by dividing the parasitemia at each 2LPC concentration by that in 0.5% Albumax. Means and SD are shown for four independent experiments. Significance relative to 3D7 was assessed for 15 to 25 μM concentrations with Welch's *t*-test. *, $P < 0.05$; **, $P < 0.01$. (*B*) QKO parasites are hypersensitive to LPC toxicity. 3D7 and QKO parasites were cultured for 48 h in complete RPMI supplemented with LPC 18:1 (1.95 to 240 μM) and parasite growth was quantified using SYBR Green. Points were fitted to a four-parameter dose–response curve. Data are from two independent experiments. (*C* and *D*) Parasites lacking XL2 and XLH4 do not proliferate in medium containing human serum. Parasite lines were grown in RPMI medium supplemented with either 0.5% Albumax I (*C*) or 10% pooled human serum (*D*). Parasitemia was determined from >1,000 RBCs on Giemsa-stained smears. Cumulative parasitemia is the parasitemia on day X multiplied by fold-subculture up to that point. Where parasite growth was observed, data were natural-log transformed and fitted by linear regression. One of two independent experiments with similar results is shown. (*E*) AKU-010 inhibits the growth of 3D7 and ΔXL2 parasites in serum but not Albumax I. Ring-stage parasites were cultured for 96 h in media containing 10% human serum or 0.5% Albumax I and AKU-010 (2.2 nM to 5 μM). Parasite growth was quantified using SYBR Green. Means and SD are from three independent experiments. Serum data points are fitted to a four-parameter dose–response curve and Albumax (Alb) data points are shown with a connecting line. (*F*) AKU-010 sensitizes 3D7 parasites to LPC in Albumax-containing medium. Ring-stage parasites were cultured for 48 h with LPC 18:1 (7.5 to 240 μM), with or without 5 μM AKU-010. Parasite growth was quantified using SYBR Green. Means and SD are from three independent experiments. Points were fitted to a four-parameter dose–response curve.

The studies in 2LPC media suggested that parasite lysophospholipases may fulfill two critical roles: generating fatty acids for lipid synthesis and protecting against LPC toxicity. To evaluate the latter role, we supplemented Albumax-containing medium with LPC 18:1 at concentrations up to 240 μM and evaluated the growth of 3D7 and QKO parasites over one cycle. QKO parasites were substantially more sensitive to LPC toxicity compared to the wild-type 3D7 line, with EC_{50} values of 33 ± 3 μM and 72 ± 5 μM, respectively (Fig. 4*B*).

All parasite lines exhibited comparable growth rates in Albumax-containing medium (Fig. 4*C*), which is likely due to the high free fatty acid and low LPC content of this serum replacement (*Discussion*). Human serum, a physiologically relevant source of exogenous fatty acids, has a substantially different composition: high concentrations of free fatty acids and LPC, both in the range of 200 to 300 μM (7). We assessed the ability of XL/XLH-deficient parasites to proliferate in media containing 10% human serum (Fig. 4*D*). Strikingly, QKO parasites were unable to replicate under these conditions. This phenotype was also observed with ΔXL2/XLH4 parasites but not with the single ΔXL2 or ΔXLH4 lines (although the ΔXLH4 line exhibited a substantially reduced growth rate), indicating that robust LPC metabolism is required for parasite growth in the presence of serum. Complementation of the QKO line with XL2 fully restored growth in serum (Fig. 4*D*).

Finally, given the inability of LPL-deficient parasites to flourish in the presence of human serum, we asked whether treatment of 3D7 and ΔXL2 parasites with the XL/XLH inhibitor AKU-010 would phenocopy the effects of XL2/XLH4 knockout. This was indeed the case (Fig. 4*E*). In Albumax-containing medium, both parasite lines were insensitive to AKU-010 concentrations up to 5 μM. In sharp contrast to this, growth of both parasite lines in serum-containing medium was inhibited with AKU-010 EC_{50} values of ~0.1 μM. To confirm that LPC is the serum constituent that sensitizes parasites to AKU-010, we conducted an LPC toxicity assay in Albumax-containing medium with and without 5 μM AKU-010 (Fig. 4*F*). The EC_{50} value dropped from 61 ± 4 μM in the absence of inhibitor to 32 ± 2 μM in the presence of 5 μM AKU-010. Notably, the latter EC_{50} value is not significantly different from that for the QKO line (Fig. 4*B*; $P = 0.70$ by Welch's *t*-test), indicating that AKU-010 is an effective inhibitor of XL/XLH activities in cultured parasites.

Discussion

We have identified two enzymes, XL2 and XLH4, that are each capable of efficient hydrolysis of exogenous LPC in asexual *P. falciparum*–infected erythrocytes (Fig. 5*A*). Knockout of either enzyme individually had a negligible effect on the ability of parasites to scavenge fatty acids from LPC; however, deletion of both enzymes greatly reduced parasite lysophospholipase activity in vitro and in situ, diminished the ability of parasites to scavenge fatty acids from LPC, and hypersensitized them to LPC toxicity (Fig. 5*B*). A low level of residual LPL activity in QKO parasites likely accounts for their ability to replicate to a reduced extent in 2LPC medium. To date, three other parasite serine hydrolases have been shown to have LPL activity in vitro (18–20) and likely contribute to residual activity. Overall, our studies are consistent with previous reports that LPC-derived fatty acids are efficiently incorporated into parasite lipids (9, 10). The glycerophosphocholine generated from LPC hydrolysis can be further hydrolyzed to glycerol-3-phosphate and choline by an essential glycerophosphoester phosphodiesterase (GDPD) that is located in the parasite's parasitophorous vacuole and cytosol (12, 39) (Fig. 5*A*). Because the parasitophorous vacuole membrane is permeable to small molecules, this distribution of GDPD positions it to hydrolyze glycerophosphocholine generated by both XL2 (in the parasitophorous vacuole) and XLH4 (in the cytosol).

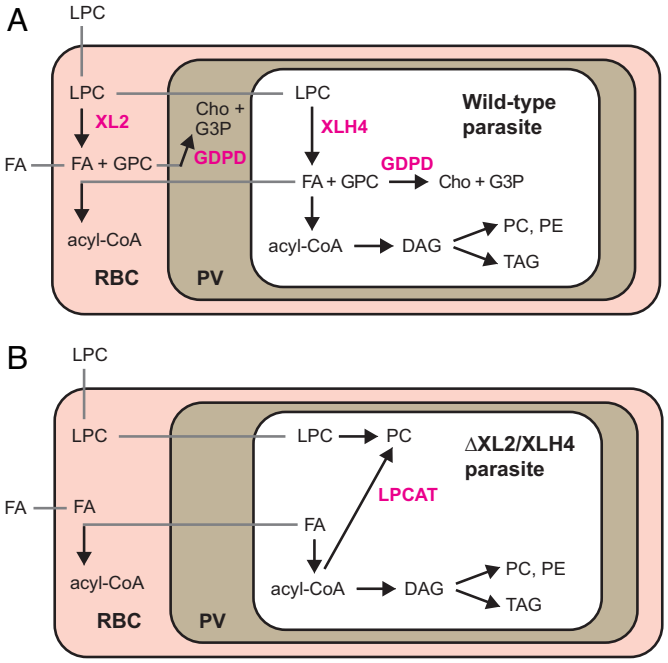

Fig. 5. LPC metabolism in *P. falciparum* and consequences of the loss of XL2 and XLH4 activities. (*A*) In wild-type parasites, LPC is hydrolyzed to fatty acids and glycerophosphocholine (GPC) either in the host erythrocyte by XL2 or within the parasite by XLH4. The liberated fatty acids (FA) serve as precursors for lipid synthesis while GPC is hydrolyzed to glycerol-3-phosphate (G3P) and choline (Cho) by glycerophosphocholine phosphodiesterase (GDPD). Exogenous fatty acids can also be taken up and incorporated into parasite lipids. Arrows indicate metabolic reactions with the corresponding enzymes in magenta and gray lines indicate transport processes. RBC, red blood cell; PV, parasitophorous vacuole. (*B*) Loss of XL2 and XLH4 greatly diminishes the rate of hydrolysis of LPC (a low level of hydrolysis is likely occurring but is not depicted). LPC accumulating in the infected erythrocyte may be directly acylated to PC through the activity of an LPC acyltransferase (LPCAT) with acyl-CoA serving as co-substrate. Exogenous free fatty acids serve as the primary FA source for parasite lipid synthesis.

We propose that XL2 catalyzes the hydrolysis of LPC in the erythrocyte cytosol. The resulting fatty acids may serve as substrates for parasite-exported acyl-CoA synthetases (40) and must also be able to enter the parasite efficiently, given the ability of XL2 complementation of the QKO line to fully restore LPC hydrolysis and growth in 2LPC medium. XL2 is not conserved across *Plasmodium* spp. but is restricted to the *Laverania* subgenus consisting of human and ape parasites. This may reflect an adaptation to the mature erythrocyte environment, as these host cells have a limited capacity for lipid metabolism. XLH4 is a cytosolic enzyme that is found in human- and ape-infecting *Plasmodium* species (including the non-Laveranian species *vivax, knowlesi, malariae,* and *ovale*) but is absent from rodent parasites (PlasmoDB.org), where LPC hydrolysis is likely catalyzed by members of the multi-gene family of serine hydrolases annotated as "lysophospholipase, putative." We speculate that XLH4 catalyzes the hydrolysis of LPC that either escapes hydrolysis in the erythrocyte or that diffuses into the parasite through points of contact between host cell and parasite membranes (41, 42). Clearly, XLH4 can compensate for the absence of extensive LPC hydrolysis in the host erythrocyte, as indicated by the minimal impact of deleting XL1 and XL2. Fatty acids generated through XLH4 activity can directly enter the parasite acyl-CoA pool and be used for parasite lipid synthesis (Fig. 5*A*). While XL2 and XLH4 appear to be functionally

redundant in culture, it is possible that they make distinctive contributions to parasite fitness in the host circulation, which contains much higher levels of LPC.

A surprising finding was the ~10-fold elevation in OA-labeled PC observed in OA/LPC competition assays with parasite lines lacking both XL2 and XLH4, with more modest elevations in the ΔXL2 and ΔXLH4 lines. The most likely explanation for this phenomenon is direct acylation of LPC, a ubiquitous reaction in eukaryotes that has not previously been described in *P. falciparum*. According to this model (Fig. 5*B*), intracellular LPC levels are elevated in the absence of XL2 and XLH4, leading to increased flux through an existing LPC acylation pathway. At least two erythrocyte enzymes have LPC acyltransferase (LPCAT) activity: LPCAT1 (43) and peroxiredoxin 6, a trifunctional human enzyme possessing LPCAT activity (44). These enzymes do not appear to be the putative LPCAT activity observed in XL2/XLH4-deficient parasite lines, however, as the levels of PC production in uninfected erythrocytes were insufficient to account for those in infected erythrocytes. Alternatively, LPCAT activity could be expressed by the parasite; the *P. falciparum* genome encodes a homolog of human LPCAT (PF3D7_0914200). Further investigation will be required to identify the relevant acyltransferase(s) and to evaluate their physiological significance in a wild-type genetic background.

Parasite LPC metabolism appears to have a dual role: i) acquisition of fatty acids and choline; and ii) protection from LPC toxicity. All XL/XLH-deficient parasites generated in this study replicated at comparable rates in medium containing Albumax, an enriched bovine serum albumin product that is relatively rich in free fatty acids (FFA) and poor in LPC. Based on literature values for the FFA and LPC content of Albumax (45), we estimate that our standard formulation of 0.5% Albumax (w/v) in RPMI provided ~66 μM FFA and ~11 μM LPC. By contrast, human serum contains high levels of both free fatty acids and LPC. A detailed analysis of the human serum metabolome revealed total FFA and LPC concentrations of 220 and 280 μM, respectively [Table 11 in Psychogios et al. (7)]. In medium with 10% (v/v) human serum, the LPC concentration would be ~28 μM. Thus, we speculate that the elevated LPC concentration in serum compared to Albumax, and possibly also the LPC:FFA ratio, were responsible for the lack of growth of ΔXL2/XLH4 and QKO parasites in serum. The growth-inhibitory properties of serum could accrue from perturbation to membranes or from dysregulation of PC synthesis in the absence of LPC metabolism. Consistent with this interpretation, wild-type and ΔXL2 parasites were sensitized to AKU-010 in serum-containing medium and wild-type parasites were hypersensitive to LPC in the presence of AKU-010. Together, these findings highlight the importance of XL/XLH-mediated LPC catabolism for parasite proliferation in high-LPC environments such as that found in the host circulation and they validate the co-inhibition of XL2 and XLH4 as a viable anti-malarial strategy.

Materials and Methods

Materials. BODIPY™ 500/510 C_4, C_9 (C4,C9-FA), and BODIPY-TR-ceramide (BTC) were obtained from ThermoFisher. LPC 18:1 and 16:0, LPE 18:1, LPS 18:1, Lyso-PAF 18:1, (*Z*)-octadec-9-en-17-ynoic acid (oleic acid alkyne), TopFluor® LPC, and TopFluor® fatty acid were obtained from Avanti Polar Lipids. IDFP and JW642 were purchased from Cayman Chemical. 3-azido-7-hydroxycoumarin was acquired from Abcam. Piperazine-based MAGL inhibitors described in Aaltonen et al. (24) were provided by Dr. T. Nevalainen, University of Eastern Finland. The following reagent was obtained through BEI Resources, NIAID, NIH: DSM1, MRA-1161. WR99210 was a gift from D. Jacobus (Jacobus Pharmaceuticals).

Parasite Culture and Transfection. *P. falciparum* clone 3D7 was routinely cultured in human O^+ erythrocytes (Interstate Blood Bank) at 2% hematocrit in RPMI 1640 medium supplemented with 0.37 mM hypoxanthine, 11 mM glucose, 27 mM sodium bicarbonate, 25 mM HEPES, 10 μg/mL gentamicin, and 5 g/L Albumax I (Gibco). Cultures were incubated at 37 °C in a 5% CO_2 incubator under normoxic conditions and were synchronized by treatment with 5% (w/v) sorbitol. Detailed methods for the generation of plasmids and for parasite transfection, selection, and validation are provided in *SI Appendix*.

C4,C9-FA Competition Assay for Inhibition of LPC Hydrolysis In Situ. Assays for inhibition of LPC hydrolysis in intact parasitized erythrocytes were conducted using a dual-fluorescent labeling strategy as previously described (21) and modified as follows. Parasites were pre-labeled with 1 μM BODIPY-TR-ceramide (BTC) in complete RPMI for 1 h. They were then washed into fatty acid-free (i.e., incomplete) RPMI, aliquoted at 0.5 mL and 8% hematocrit into a 24-well plate, supplemented with 10 μM inhibitor or equivalent volume of DMSO, and incubated for 30 min at 37 °C in a CO_2 incubator. An equal volume of medium containing fatty acid–free BSA, C4,C9-FA, LPC18:1 (or 50% ethanol for no-LPC controls), and 10 μM inhibitor (or DMSO for no-inhibitor controls) was added, such that final concentrations were 2 mg/mL BSA, 30 μM C4,C9-FA, 30 μM LPC18:1 and 10 μM inhibitor. After 30 min, cultures were transferred to 9 mL of cold 0.03% saponin in PBS and parasites were isolated by centrifugation. Lipids were extracted as previously described (21), dissolved in chloroform, and spotted on a 10- × 10-cm glass HPTLC Silica Gel 60 plate (Millipore). BTC fluorescence was imaged on a Typhoon RGB imager (Cytiva) using a 633-nm laser and a 670/30 bandpass filter. Neutral lipids were resolved in heptane/diethyl ether/acetic acid at a ratio of 40:60:1 and C4,C9-FA fluorescence was imaged using the 532 nm laser and a 570/20 bandpass filter. Fluorescence intensities for DAG, TAG, and BTC were quantified using ImageQuantTL (Cytiva). BTC fluorescence intensities were used to normalize DAG and TAG intensities across samples.

XLH4-YFP/HA Localization. Live parasites expressing XLH4-YFP were imaged by mounting an aliquot of culture under a coverslip. Parasites expressing XLH4-HA were fixed with 2% paraformaldehyde and 0.0065% glutaraldehyde in PBS, permeabilized with 0.1% Triton-X100, and incubated with monoclonal anti-HA antibody 16B12 (Covance, 2 μg/mL) followed by anti-mouse Alexa488-conjugated secondary antibody (ThermoFisher, 2 μg/mL). Hoechst 33342 was added to 2 μM to visualize DNA. Images were collected on a Zeiss Axioimager M1 epifluorescence microscope with a 100x/1.4 NA objective. Contrast was adjusted using Adobe Photoshop.

MACS Purification and TAMRA-FP Analysis. Parasites were enriched from ~100 mL of culture containing synchronized schizonts (~36 to 44 h post-invasion) at ~10% parasitemia using a SuperMACS™ II Separator and a D Column (Miltenyi Biotec). Numbers of eluted cells were determined with a hemocytometer and parasitemia was calculated from a Giemsa-stained smear. Typical yields were 5×10^8 parasite-infected erythrocytes at 90 to 95% parasitemia. To generate cell lysates, pellets were resuspended at 5×10^8 parasites/mL in cold PBS supplemented with 5 μM pepstatin A and 10 μM E64. The suspension was sonicated three times for 8 s using a microtip at 30% maximum power. Hemozoin was removed by centrifugation at 12,000×*g* at 4 °C. Lysates were aliquoted, snap frozen in liquid nitrogen, and stored at −80 °C. Lysates of uninfected erythrocytes (uRBC) were generated in the same manner except that the MACS separation was omitted.

For serine hydrolase inhibitor profiling with the activity-based probe TAMRA-FP, 19.4 μL of MACS or uRBC lysate was mixed with 0.2 μL of 1 mM inhibitor (or DMSO for controls) and 0.2 μL of 100 μM AA74-1 to selectively inhibit human APEH (27), and was incubated at 30 °C for 30 min. Probe labeling was conducted by adding 0.2 μL of 100 μM TAMRA-FP and incubating at 30 °C for 30 min. The reaction was quenched by adding 20 μL of 2X SDS–PAGE loading buffer and incubating at 95 °C for 5 min. Labeled proteins were resolved on 8.5 or 10% sodium dodecyl sulfate–polyacrylamide gels and imaged on a Typhoon RGB flatbed scanner using the 532 nm laser and a 570/20 bandpass filter.

Oleate Alkyne Competition Assay for Inhibition of LPC Hydrolysis In Situ. Synchronized parasite cultures with ~10% trophozoites were labeled with 1 μM BTC for 1 h at 37 °C in a CO_2 incubator and then washed three times with

incomplete RPMI. Cultures were resuspended in pre-warmed incomplete RPMI containing 3 mg/mL fatty acid-free BSA, 30 μM oleic acid alkyne, and 30 μM LPC 18:1 (or 50% ethanol for no-LPC controls) and incubated for 40 min with gentle mixing on an orbital rotator at 37 °C in a CO_2 incubator. Labeled cultures were harvested and lipids were extracted as described above for C4,C9-FA competition assays. Alkyne-labeled lipids were rendered fluorescent by Cu-catalyzed azide–alkyne cycloaddition of 3-azido-7-hydroxycoumarin as previously described (31). Solvent was evaporated in a vacuum centrifuge and lipids were redissolved in ~10 μL chloroform. For TLC separation, 1 μL was spotted on a 10 cm × 10 cm glass HPTLC Silica Gel 60 plate (Millipore). BODIPY-TR-ceramide fluorescence was then recorded as described above for C4,C9-FA competition assays. Phospholipids were developed with 65:25:4:1 chloroform/methanol/water/acetic acid for about 4.5 cm. Plates were air dried and neutral lipids were resolved with 1:1 hexane/ethyl acetate. Plates were sprayed with 6 mL 4% (v/v) *N*,*N*-diisopropylethylamine in hexane prior to imaging. Fluorescence was imaged on an Azure C400 CCD camera imager using blue LED illumination (472 nm) for excitation and a 513/17 nm bandpass filter for emission. BTC, neutral, and polar lipid fluorescence intensities were quantified using ImageQuantTL software (Cytiva), and lipid intensities were normalized across samples using BTC fluorescence. Competition for OA incorporation was quantified as the ratio of lipid fluorescence in +LPC and −LPC samples.

In Vitro LPC Hydrolysis Assays. Lysates of MACS-purified infected erythrocytes or of uRBC were serially threefold diluted with cold PBS. TopFluor LPC was added to 50 μM from a 2.5 mM DMSO stock, and reactions were incubated at 30 °C for 15 min. Reaction products were extracted by transferring 3 μL to 150 μL chloroform and vortexing for 20 s. Then, 1 μL of the chloroform layer was spotted on a 10- × 10-cm aluminum HPTLC Silica Gel 60 plate (Millipore). TopFluor LPC and the hydrolysis product TopFluor fatty acid were resolved with 65:25:4:1 chloroform/methanol/water/acetic acid and imaged on a Typhoon RGB scanner using a 488-nm laser and 525/20 bandpass filter. The relative fluorescence intensities of TopFluor LPC and TopFluor fatty acid were assessed by resolving equimolar mixtures using the TLC system described above and quantifying fluorescence intensities. The signal for TopFluor fatty acid was 1.25-fold higher than that for TopFluor LPC; therefore, a correction factor was applied. Percent hydrolysis was then calculated for each sample.

Growth in Medium Containing LPC as Sole Source of Fatty Acids. Synchronized ring-stage parasite cultures (0 to 16 h post-invasion) were washed three times with incomplete RPMI, resuspended at 3% parasitemia and 1% hematocrit in 1 mL of RMPI containing 3 mg/mL fatty acid-free BSA and 0 to 50 μM each of LPC 16:0 and 18:1, and placed in a 24-well plate. Parallel cultures for normalization were set up with the standard culture medium, i.e., RPMI supplemented with 0.5% Albumax I. Parasites were cultured for 60 h at 37 °C in a 5% CO_2 incubator, at which point Giemsa-stained smears were prepared. Parasitemia was calculated from a minimum of 1,000 cells.

Growth in Medium Containing Human Serum. Synchronized ring-stage parasite cultures (0 to 16 h post-invasion) at 1% parasitemia and 2% hematocrit were washed into complete RPMI containing either 0.5% Albumax I or 10% (v/v) pooled, heat-inactivated human serum (Interstate Blood Bank) and cultured at 37 °C in a 5% CO_2 incubator. Over an 8-d period, parasitemia was counted from Giemsa-stained smears (minimum 1,000 cells) every 2 d, and parasites were subcultured unless they were not thriving, in which case the medium was changed.

EC_{50} Measurements. EC_{50} values for LPC 18:1 and AKU-010 were determined using a SYBR Green I assay as previously described (46). For LPC toxicity assays, early ring stage 3D7 and QKO parasites (0 to 8 h post-invasion) were inoculated into 96-well plates at 3% parasitemia, 1% hematocrit in complete RPMI containing 0.5% Albumax I. LPC 18:1 (1.9 to 240 μM) or 50% ethanol (final concentration 0.2%) were then added, and cultures were incubated for 48 h. No hemolysis was observed under these conditions. To evaluate AKU-010 toxicity in serum, ring stage 3D7 and ΔXL2 parasites were inoculated in complete RPMI containing 0.5% (w/v) Albumax I or 10% (v/v) pooled human serum. AKU-010 (2 nM to 5 μM), DMSO (0.2%), or mefloquine (300 nM; positive control for parasite killing) were then added and cultures were incubated for 96 h. To evaluate the effect of AKU-010 on LPC toxicity, ring-stage 3D7 parasites were cultured in Albumax I-containing media with and without 5 μM AKU-010 and with 7.5 to 240 μM LPC 18:1 for 48 h. For all assays, cultures were developed with SYBR Green I as previously described (46) and fluorescence was quantified on a Molecular Devices SpectraMax M5 microplate fluorometer. Fluorescence values were expressed as a fraction of the DMSO control and the EC_{50} values were determined using four-parameter sigmoidal non-linear regression.

Data, Materials, and Software Availability. All study data are included in the article and/or *SI Appendix*.

ACKNOWLEDGMENTS. We are grateful to Tapio Nevalainen (University of Eastern Finland) for providing monoacylglycerol lipase inhibitors, Josh Beck (University of Iowa) for the CRISPR/Cas9 plasmids, and Sean Prigge (Johns Hopkins University) for pKD-PfAUBL. M.K. discloses support for this work from NIH grant AI133136 and from U.S. Department of Agriculture, National Institute of Food and Agriculture HATCH project VA-160082.

1. WHO, *World Malaria Report* (WHO, 2022).
2. M. Dhorda, C. Amaratunga, A. M. Dondorp, Artemisinin and multidrug-resistant *Plasmodium falciparum*–A threat for malaria control and elimination. *Curr. Opin. Infect. Dis.* **34**, 432–439 (2021).
3. H. J. Vial, M. L. Ancelin, "Malarial lipids" in *Malaria: Parasite Biology, Biogenesis, Protection*, I. W. Sherman, Ed. (American Association of Microbiology Press, Washington, DC, 1998).
4. N. M. Q. Palacpac *et al.*, Developmental-stage-specific triacylglycerol biosynthesis, degradation and trafficking as lipid bodies in *Plasmodium falciparum*-infected erythrocytes. *J. Cell Sci.* **117**, 1469–1480 (2004).
5. K. E. Jackson *et al.*, Food vacuole-associated lipid bodies and heterogeneous lipid environments in the malaria parasite, *Plasmodium falciparum*. *Mol. Microbiol.* **54**, 109–122 (2004).
6. A. M. Vaughan *et al.*, Type II fatty acid synthesis is essential only for malaria parasite late liver stage development. *Cell. Microbiol.* **11**, 506–520 (2009).
7. N. Psychogios *et al.*, The human serum metabolome. *PLoS ONE* **6**, e16957 (2011).
8. S. Switzer, H. A. Eder, Transport of lysolecithin by albumin in human and rat plasma. *J. Lipid Res.* **6**, 506–511 (1965).
9. H. J. Vial, M. L. Ancelin, M. J. Thuet, J. R. Philippot, Phospholipid metabolism in *Plasmodium*-infected erythrocytes: Guidelines for further studies using radioactive precursor incorporation. *Parasitology* **98**, 351–357 (1989).
10. N. M. B. Brancucci *et al.*, Lysophosphatidylcholine regulates sexual stage differentiation in the human malaria parasite *Plasmodium falciparum*. *Cell* **171**, 1532–1544 (2017).
11. H. Asahi, T. Kanazawa, N. Hirayama, Y. Kajihara, Investigating serum factors promoting erythrocytic growth of *Plasmodium falciparum*. *Exp. Parasitol.* **109**, 7–15 (2005).
12. A. Ramaprasad *et al.*, A choline-releasing glycerophosphodiesterase essential for phosphatidylcholine biosynthesis and blood stage development in the malaria parasite. *eLife* **11**, e82207 (2022).
13. R. Zidovetzki, I. W. Sherman, J. Prudhomme, J. Crawford, Inhibition of *Plasmodium falciparum* lysophospholipase by anti-malarial drugs and sulphydryl reagents. *Parasitology* **108**, 249–255 (1994).
14. A. Wang, E. A. Dennis, Mammalian lysophospholipases. *Biochim. Biophys. Acta* **1439**, 1–16 (1999).
15. J. A. Wepy *et al.*, Lysophospholipases cooperate to mediate lipid homeostasis and lysophospholipid signaling. *J. Lipid Res.* **60**, 360–374 (2019).
16. D. Davison, S. Howell, A. P. Snijders, E. Deu, Activity-based protein profiling of human and plasmodium serine hydrolases and interrogation of potential antimalarial targets. *iScience* **25**, 104996 (2022).
17. R. Elahi *et al.*, Functional annotation of serine hydrolases in the asexual erythrocytic stage of *Plasmodium falciparum*. *Sci. Rep.* **9**, 17532 (2019).
18. M. Asad *et al.*, An essential vesicular-trafficking phospholipase mediates neutral lipid synthesis and contributes to hemozoin formation in *Plasmodium falciparum*. *BMC Biol.* **19**, 159 (2021).
19. P. K. Sheokand, M. Narwal, V. Thakur, A. Mohmmed, GlmS mediated knock-down of a phospholipase expedite alternate pathway to generate phosphocholine required for phosphatidylcholine synthesis in *Plasmodium falciparum*. *Biochem. J.* **478**, 3429–3444 (2021).
20. P. K. Sheokand *et al.*, A *Plasmodium falciparum* lysophospholipase regulates host fatty acid flux via parasite lipid storage to enable controlled asexual schizogony. *Cell Rep.* **42**, 112251 (2023).
21. C. Dapper, J. Liu, M. Klemba, Leveraging a fluorescent fatty acid probe to discover cell-permeable inhibitors of *Plasmodium falciparum* glycerolipid biosynthesis. *Microbiol. Spectr.* **10**, e0245622 (2022).
22. D. K. Nomura *et al.*, Activation of the endocannabinoid system by organophosphorus nerve agents. *Nat. Chem. Biol.* **4**, 373–378 (2008).
23. J. W. Chang *et al.*, Highly selective inhibitors of monoacylglycerol lipase bearing a reactive group that is bioisosteric with endocannabinoid substrates. *Chem. Biol.* **19**, 579–588 (2012).
24. N. Aaltonen *et al.*, Piperazine and piperidine triazole ureas as ultrapotent and highly selective inhibitors of monoacylglycerol lipase. *Chem. Biol.* **20**, 379–390 (2013).
25. M. P. Patricelli, D. K. Giang, L. M. Stamp, J. J. Burbaum, Direct visualization of serine hydrolase activities in complex proteomes using fluorescent active site-directed probes. *Proteomics* **1**, 1067–1071 (2001).
26. C. Ribaut *et al.*, Concentration and purification by magnetic separation of the erythrocytic stages of all human *Plasmodium* species. *Malar. J.* **7**, 45 (2008).
27. R. Elahi, C. Dapper, M. Klemba, Internalization of erythrocyte acylpeptide hydrolase is required for asexual replication of *Plasmodium falciparum*. *mSphere* **4**, e00077-19 (2019).
28. N. J. Spillman, V. K. Dalmia, D. E. Goldberg, Exported epoxide hydrolases modulate erythrocyte vasoactive lipids during *Plasmodium falciparum* infection. *mBio* **7**, e01538-16 (2016).
29. X. Zhang *et al.*, Rapid antigen diversification through mitotic recombination in the human malaria parasite *Plasmodium falciparum*. *PLoS Biol.* **17**, e3000271 (2019).

30. E. S. Istvan *et al.*, Esterase mutation is a mechanism of resistance to antimalarial compounds. *Nat. Commun.* **8**, 14240 (2017).
31. C. Thiele *et al.*, Tracing fatty acid metabolism by click chemistry. *ACS Chem. Biol.* **7**, 2004–2011 (2012).
32. J. A. Boddey, R. L. Moritz, R. J. Simpson, A. F. Cowman, Role of the *Plasmodium* export element in trafficking parasite proteins to the infected erythrocyte. *Traffic* **10**, 285–299 (2009).
33. J. Birnbaum *et al.*, A genetic system to study *Plasmodium falciparum* protein function. *Nat. Methods* **14**, 450–456 (2017).
34. E. Soupene, H. Fyrst, F. A. Kuypers, Mammalian acyl-CoA: Lysophosphatidylcholine acyltransferase enzymes. *Proc. Natl. Acad. Sci. U.S.A.* **105**, 88–93 (2008).
35. F. Mi-Ichi, S. Kano, T. Mitamura, Oleic acid is indispensable for intraerythrocytic proliferation of *Plasmodium falciparum*. *Parasitology* **134**, 1671–1677 (2007).
36. F. Mi-Ichi, K. Kita, T. Mitamura, Intraerythrocytic *Plasmodium falciparum* utilize a broad range of serum-derived fatty acids with limited modification for their growth. *Parasitology* **133**, 399–410 (2006).
37. T. Sato, T. Fujii, Changes in shape and osmotic resistance of human erythrocytes resulted from changes in the lysolecithin content of the membranes. *Chem. Pharm. Bull* **22**, 152–156 (1974).
38. T. J. Bierbaum, S. R. Bouma, W. H. Huestis, A mechanism of erythrocyte lysis by lysophosphatidylcholine. *Biochim. Biophys. Acta* **555**, 102–110 (1979).
39. T. Denloye, S. Dalal, M. Klemba, Characterization of a glycerophosphodiesterase with an unusual tripartite distribution and an important role in the asexual blood stages of *Plasmodium falciparum*. *Mol. Biochem. Parasitol.* **186**, 29–37 (2012).
40. M. Tellez, F. Matesanz, A. Alcina, The C-terminal domain of the *Plasmodium falciparum* acyl-CoA synthetases PfACS1 and PfACS3 functions as ligand for ankyrin. *Mol. Biochem. Parasitol.* **129**, 191–198 (2003).
41. H. G. Elmendorf, K. Haldar, *Plasmodium falciparum* exports the Golgi marker sphingomyelin synthase into a tubovesicular network in the cytoplasm of mature erythrocytes. *J. Cell Biol.* **124**, 449–462 (1994).
42. P. A. Tamez *et al.*, An erythrocyte vesicle protein exported by the malaria parasite promotes tubovesicular lipid import from the host cell surface. *PLoS Pathog.* **4**, e1000118 (2008).
43. E. Soupene, V. Serikov, F. A. Kuypers, Characterization of an acyl-coenzyme A binding protein predominantly expressed in human primitive progenitor cells. *J. Lipid Res.* **49**, 1103–1112 (2008).
44. A. B. Fisher *et al.*, A novel lysophosphatidylcholine acyl transferase activity is expressed by peroxiredoxin 6. *J. Lipid Res.* **57**, 587–596 (2016).
45. F. R. Garcia-Gonzalo, J. C. Izpisua Belmonte, Albumin-associated lipids regulate human embryonic stem cell self-renewal. *PLoS ONE* **3**, e1384 (2008).
46. M. Smilkstein, N. Sriwilaijaroen, J. X. Kelly, P. Wilairat, M. Riscoe, Simple and inexpensive fluorescence-based technique for high-throughput antimalarial drug screening. *Antimicrob. Agents Chemother.* **48**, 1803–1806 (2004).